Spontaneous emission lifetime of carriers in a semiconductor microcavity measured by photoluminescence without distortion by reabsorption

S. Park, V. Zapasskii[#], D. V. Wick[*], T. R. Nelson, Jr.[+], C. Ell, H. M. Gibbs, G. Khitrova and A. Schülzgen
Optical Sciences Center, University of Arizona, Tucson, AZ 85721
sahnggi@optics.Arizona.EDU, gibbs@.optics.Arizona.EDU

M. Kira, F. Jahnke and S. W. Koch
Department of Philipps-University Marburg, 35032 Marburg, Germany
Physics and Material Sciences Center

[#] Also: Vavilov State Optical Institute, St.- Petersburg, 199034, Russia
[*] Present address: Air Force Research Laboratory/DEBS, 3550 Aberdeen Ave. SE, Kirtland AFB, NM 87117
[+] Present address: Electron Devices Branch, Sensors Directorate, Air Force Research Laboratory (AFRL/SNDD), Wright-Patterson Air Force Base, OH- 45433-7322

Abstract: A theory for carrier decay rates and a technique for measuring them are reported. Modification of the spontaneous emission rate of carriers by a semiconductor microcavity is investigated with 100-nm-thick bulk GaAs. Reabsorption makes the cavity-mode photoluminescence (PL) decay much faster than the square of the carrier density. Here reabsorption distortion is avoided by collecting PL that escapes the microcavity directly without multiple reflections: a ZnSe prism glued to the top mirror allows PL to escape at angles beyond the cutoff angle for total internal reflection without the prism. At these steep angles, the stop band of the top mirror has shifted to higher energy, so that it does not impede PL emission. Removal of most of the bottom mirror decreases the true carrier decay rate by only ≈25%, showing that the large enhancements deduced from cavity-mode PL are incorrect. Fully quantum mechanical computation including guided modes corroborates this conclusion. The prism technique could be used to study carrier dynamics and competition between guided and cavity modes in microcavities below and near threshold.

OCIS codes: (260.3800) Luminescence; (310.2790) Guided waves; (999.9999) spontaneous emission decay rates

References and links

1. P. Goy, J. M. Raimond, M. Gross, and S. Haroche, "Observation of cavity-enhanced single-atom spontaneous emission," Phys. Rev. Lett. **50**, 1903-1906 (1983).
2. S. Haroche and J. M. Raimond, "Radiative properties of Rydberg states in resonant cavities," 347-411 in B. Bederson and D. R. Bates, eds., *Advances in Atomic and Molecular Physics 20* (Academic, New York, 1985).
3. H. J. Kimble, "Structure and dynamics in cavity quantum electrodynamics," 203-266 in P. R. Berman, ed., *Cavity Quantum Electrodynamics* (Academic, Boston, 1994).
4. M. Kira, F. Jahnke, and S. W. Koch, "Microscopic theory of excitonic signatures in semiconductor photoluminescence," Phys. Rev. Lett. **81**, 3263-3266 (1998).
5. L. C. Andreani, F. Tassone, and F. Bassani, "Radiative lifetime of free excitons in quantum wells," Solid State Commun. **77**, 641-645 (1991).
6. D. S. Citrin, "Radiative lifetimes of excitons in semiconductor quantum wells," Comments Cond. Mat. Phys. **16**(5), 263-280 (1993).

#10797 - $15.00 US Received April 23, 1999; Revised June 15, 1999

7. C. Weisbuch, M. Nishioka, A. Ishikawa, and Y. Arakawa, "Observation of the coupled exciton-photon mode splitting in a semiconductor quantum microcavity," Phys. Rev. Lett. **69**, 3314-3317 (1992).
8. G. Khitrova, H. M. Gibbs, F. Jahnke, M. Kira, and S. W. Koch, "Nonlinear optics of normal-mode-coupling semiconductor microcavities," Rev. Mod. Phys., to be published.
9. M. Kira, F. Jahnke, W Hoyer, and S. W. Koch, "Quantum theory of spontaneous emission and coherent effects in semiconductor microstructures," Prog. Quantum Electron., to be published.
10. M. Kira, F. Jahnke, S. W. Koch, J. D. Berger, D. V. Wick, T. R. Nelson, Jr., G. Khitrova, and H. M. Gibbs, "Quantum theory of nonlinear semiconductor microcavity luminescence explaining "Boser" experiments," Phys. Rev. Lett. **79**, 5170-5173 (1997).
11. E. M. Purcell, "Spontaneous emission probabilities at radio frequencies," Phys. Rev. **69**, 681 (1946).
12. *Cavity Quantum Electrodynamics*, edited by P. R. Berman, (Academic Press, New York, 1994).
13. G. Björk, S. Machida, and K. Igata, "Modification of spontaneous emission rate in planar dielectric microcavity structures," Phys. Rev. A, **44**, 669-681 (1991).
14. Y. Yamamoto, S. Machida, Y. Horikoshi, K. Igeta, and G. Björk, "Enhanced and inhibited spontaneous emission of free excitons in GaAs quantum wells in a microcavity," Opt. Commun. **80**, 337-342 (1991).
15. D. L. Huffaker, C. Lei, D. G. Deppe, C. J. Pinzone, J. G. Neff, and R. D. Dupuis, "Controlled spontaneous emission in room-temperature semiconductor microcavities," Appl. Phys. Lett. **60**, 3203-3205 (1992).
16. K. Tanaka, T. Nakamura, W. Takamatsu, M. Yamanishi, Y. Lee, and T. Ishihara, "Cavity-induced changes of spontaneous emission lifetime in one-dimensional semiconductor microcavities," Phys. Rev. Lett. **74**, 3380-3383 (1995).
17. L. A. Graham, D. L. Huffaker, Q. Deng, and D. G. Deppe, "Controlled spontaneous lifetime in microcavity confined InGaAlAs/GaAs quantum dots," Appl. Phys. Lett. **72**, 1670-1672 (1998).
18. R. Jin, M. S. Tobin, R. P. Leavitt, H. M. Gibbs, G. Khitrova, D. Boggavarapu, O. Lynnes, E. Lindmark, F. Jahnke, and S. W. Koch, "Order of magnitude enhanced spontaneous emission from room-temperature bulkGaAs," in *Microcavities and Photonic Bandgaps: Physics and Applications*, J. Rarity, and C. Weisbuch, ed. (Kluwer, Dordrecht,1996), p. 43.
19. H. K. Yokoyama, K. Nishi, T. Anan, H. Yamada, S. D. Brorson, and E. P. Ippen, "Enhanced spontaneous emission from GaAs quantum wells in monolithic microcavities," Appl. Phys. Lett. **57**, 2814-2816 (1990).
20. Y. Hanamaki, H. Kinoshita, H. Akiyama, N. Ogasawara, and Y. Shirki, "Spontaneous emission lifetime alteration in InGaAs/GaAs vertical-cavity surface-emitting laser structures," Phys. Rev. B **56**, R4379-4382 (1997).
21. C. C. Lin, D. G. Deppe, and C. Lei, "Role of waveguide light emission in planar microcavities," IEEE J. Quantum Electron. **30**, 2304-2312 (1994).
22. Analysis shows that reabsorption distortion can be avoided if a stationary carrier density is maintained in the active layer, e.g., by means of cw pumping. In this case, PL dynamics of this sample subjected to a weak perturbation (e.g., to a short pump pulse) will exactly reproduce dynamics of carriers (provided that the perturbation is sufficiently small).
23. I. Abram, S. Iung, R. Kuszelewicz, G. Le Roux, C. Licoppe, J. L. Oudar, and E. V. K. Rao, "Nonguiding half-wave semiconductor microcavities displaying the exciton-photon mode splitting," Appl. Phys. Lett. **65**, 2516-2518 (1994).
24. E. F. Schubert, N. E. J. Hunt, M. Micovic, R. J. Malik, D. L. Sivco, A. Y. Cho, and G. J. Zydzik, "Highly efficient light-emitting diodes with microcavities," Science **265**, 943-945 (1994).
25. H. De Neve, J. Blondelle, R. Baets, P. Demeester, P. Van Daele, and G. Borghs, "High efficiency planar microcavity LED's: comparison of design and experiment," IEEE Phot. Tech. Lett. **7**, 287-289 (1995).
26. H. De Neve, J. Blondelle, P. Van Daele, P. Demeester, R. Baets, and G. Borghs, "Recycling of guided mode light emission in planar microcavity light emitting diodes," Appl. Phys. Lett. **70**, 799-801 (1997).
27. H. Rigneault, S. Robert, C. Begon, B. Jacquier, and P. Moretti, "Radiative and guided wave emission of Er^{3+} atoms located in planar multidielectric structures," Phys. Rev. A **55**, 1497-1502 (1997).
28. H. Rigneault, S. Robert, C. Amra, F. Lamarque, S. Monneret, B. Jacquier, P. Moretti, A. M. Jurdyc, and A. Belarouci, "Spontaneous emission of rare earth ions confined in planar multilayer dielectric microcavities," SPIE **3133**, 78-87 (1997).
29. R. P. Stanley, R. Houdré, C. Weisbuch, U. Oesterle, and M. Ilegems, "Cavity-polariton photoluminescence in semiconductor microcavities: experimental evidence," Phys. Rev. B **53**, 10995-11007 (1996).
30. E. Spiller, "Saturable resonator for visible light," J. Opt. Soc. Am. **61**, 669 (1971) and "Saturable optical resonator," J. Appl. Phys. **43**, 1673-1681 (1972).
31. D. L. Huffaker and D. G. Deppe, "Spontaneous coupling to planar and index-confined quasimodes of Fabry-Pérot microcavities," Appl. Phys. Lett. **67**, 2594-2596 (1995).
32. D. G. Deppe, T. -H. Oh, and D. L. Huffaker, "Eigenmode confinement in the dielectrically apertured Fabry-Perot microcavity," IEEE Photon. Tech. Lett. **9**, 713-715 (1997).
33. F. Jahnke, M. Kira, and S. W. Koch, "Linear and nonlinear optical properties of excitons in semiconductor quantum well and microcavities," Z. Physik B **104,** 559-572 (1997).
34. J. M. Gérard, B. Sermage, B. Gayral, B. Legrand, E. Costard, and V. Thierry-Mieg, "Enhanced spontaneous emission by quantum boxes in a monolithic optical microcavity", Phys. Rev. Lett. **81**, 1110-1113 (1998).

#10797 - $15.00 US Received April 23, 1999; Revised June 15, 1999

1. Introduction

The elementary atom-photon interaction is strongly modified when an atom is confined to a small cavity. Atomic cavity QED is a mature and well-understood field. There are two regimes, perturbative and nonperturbative. In the perturbative regime, spontaneous emission is enhanced or inhibited due to a modification of the photon density of states, and it is irreversible; photons leave the cavity rapidly. The decay rate is increased as $\Gamma_{cav} \approx \Gamma_0 Q\lambda^3/V$, where $Q = \omega/\Delta\omega_{cav}$ and V is the cavity-mode volume. The spontaneous emission rate has been increased by a factor of 500 in the microwave regime [1]. By decreasing V further (mostly by decreasing the cavity length), one can reach the nonperturbative regime; a photon stays in the cavity for a rather long time, being emitted and absorbed by atoms several times. This is reversible spontaneous emission, and one can observe vacuum Rabi oscillations and vacuum Rabi splitting (normal-mode coupling) [2,3].

Semiconductor cavity QED is understood less well, because of the complexities of planar semiconductor microcavities. First, exciting into the continuum and producing electron-hole pairs is very different from exciting resonantly and producing excitons. Second, there is growing theoretical evidence that electrons and holes generated by continuum excitation recombine without forming excitons; a PL peak at the exciton resonance does not imply more than one exciton [4]. Third, electron-hole spontaneous emission in bulk material relies on surfaces, impurities, or carrier collisions to conserve momentum, so it is relatively slow (≈1 ns). In contrast, the radiative lifetime of a quantum-well exciton is typically 10-20 ps for resonant excitation; a photon can carry away all of the in-plane center-of-mass momentum [5,6]. Since observed PL decay times for nonresonant excitation are much longer than the fast exciton radiative lifetime for resonant excitation, a correct treatment of PL must follow electron and hole distributions and not use a fixed-dipole approximation. Cooling to quasi-equilibrium electron and hole distributions need not be computed, since it is much faster than electron-hole radiative recombination at below-transparency carrier densities. In the nonperturbative regime [7] reversible spontaneous emission oscillations occur only if the system is excited resonantly. Nonresonant excitation results only in electron-hole recombination, mostly into guided modes. At present the nonperturbative regime with nonresonant excitation is much better understood in semiconductors than the perturbative regime [8].

In this paper we present measurements and calculations of the spontaneous emission lifetime with nonresonant excitation. We show that the large enhancement of the cavity-mode PL decay rate with increased mirror quarterwave pairs is not a cavity-QED effect but a shuttering action of the nonlinear cavity as the absorption recovers. Measurements with a prism permitting observation of PL into the guided modes made it possible to unravel the origin of the mystery.

We have developed the ability to compute spontaneous emission with nonresonant pumping [9]. It has been used successfully in "Boser" calculations [10] and here. It is confirmed that a relatively large fraction of the spontaneously emitted light is channeled into the guided modes and thus not available for emission in the normal direction.

Since the prediction that the spontaneous emission of an atom is not an immutable property, but can be altered by a cavity around it [11,12], many experimental and theoretical works have investigated controlled spontaneous emission of atoms, rare-earth ions, dye molecules, semiconductors, etc. In cavity-QED, spontaneous emission is viewed as a decay process of an excited atom, stimulated by vacuum field fluctuations. The decay rate is given by Fermi's golden rule, $\Gamma \propto |< \mathbf{d}\cdot\mathbf{E} >|^2 \rho(\omega)$; $\mathbf{d}$ and $\mathbf{E}$ are the electric dipole operator of an atom and the electric field operator at the position of the atom, respectively, and $\rho(\omega)$ is the photon mode density per unit energy. It is clear that the decay rate can be altered either by changing the electric field at the location of the emitter, or by changing the mode density [11-13]. In a cavity both the mode density and the vacuum field strength are different from those in free space, leading to an enhanced or inhibited decay rate. The possibility of spontaneous

#10797 - $15.00 US Received April 23, 1999; Revised June 15, 1999

emission controlled by a semiconductor microcavity has attracted a lot of interest with the prospect of improving light emitting diode (LED) performance and lowering the threshold of a vertical-cavity surface-emitting laser (VCSEL).

The control of spontaneous emission by a semiconductor microcavity has been studied with various emitters: bulk, quantum wells, quantum dots. Strong microcavity modifications of the angular distribution and spectral shape of the emission of low-density cold excitons was reported by Yamamoto et al. [14]. Huffaker et al. [15] observed similar controlled-spontaneous-emission alterations of the angular distribution at room temperature. Tanaka et al. [16] observed a 36% enhancement in the emission rate following continuum excitation of a single 10-nm GaAs quantum well inside a microcavity at 30 K. Using InGaAlAs quantum dots, Graham et al. [17] found a ≈30% faster decay following continuum excitation when the cavity peak was lower in energy compared with higher in energy than the exciton resonance. Both [16] and [17] claim agreement with oriented atomic dipole theory.

However, the fixed-dipole theory cannot describe cavity enhancement effects due to many relevant phenomena in semiconductors like the rapid momentum-changing carrier-carrier scattering within an electron-hole plasma. It is well known that a semiconductor laser can have a very high efficiency even though the wavelength region over which there is gain is much broader than the cavity linewidth. As stimulated emission tries to burn a spectral hole to saturate the gain locally, very rapid carrier-carrier collisions fill in the hole by scattering in carriers having other momenta. The situation is again different when the carrier density is so low that there is no gain at all, as might be the case for very low-power LEDs. In [18], it was shown theoretically that, *if* the principal decay channel is one or more modes enhanced by the cavity, then carrier-carrier scattering ensures that the carrier decay is enhanced by the cavity. In that case a microcavity enhancement much larger than for fixed dipoles could occur.

In 1990, Yokoyama et al. [19] performed experiments on three 6.5-nm GaAs quantum wells in a low-index $\lambda/2$ spacer grown on top of an R = 0.98 twenty-pair AlAs/AlGaAs bottom mirror, observing PL with and without an R = 0.9 seven-layer ZnS/SiO_2 dielectric top mirror. They found that the initial decay rate following picosecond excitation to a density just below transparency at 300 K was a factor of two faster for quantum wells inside a microcavity than for quantum wells with no microcavity.

In 1996, Jin et al. [18] reported an order of magnitude enhancement of the spontaneous emission rate at 300 K for a 100-nm-thick layer of bulk GaAs embedded in the center of a microcavity. Rather similar results were reported in [20]. However, in a high-reflectivity microcavity as studied in [18,20] and here, reabsorption of cavity-mode PL and the large density of states of guided modes [21] cause the dominant decay channel to be guided modes. Since the cavity does not enhance radiative recombination into guided modes, there is little enhancement of the carrier decay rate. The mistake in [18], and presumably in [20], was assuming that the cavity-mode PL decay is the same as the decay of $f_e f_h$, the product of the electron and hole distribution functions. As discussed below reabsorption within the emitting GaAs layer in effect closes a shutter on the cavity-mode PL, making its decay much faster than that of $f_e f_h$.

The experiment here shows that it is almost impossible to deduce the carrier decay curve directly from the decay of the cavity-mode PL in a high-reflectivity microcavity following short-pulse excitation [22]. This is because the emitting-layer absorption increases as the carriers decay, drastically reducing the fraction of the cavity-mode PL that escapes. As this absorption increases with time, the probability of reabsorption of the cavity-mode PL also increases, so the probability that cavity-mode PL escapes decreases. Clearly the chance that reabsorbed PL is re-emitted into the cavity mode is just as small as for the direct PL. Thus, when measuring PL dynamics in the cavity mode, we actually detect the intensity of the PL transmitted through a filter with a strongly density and thus time-dependent transmission.

The pronounced effect of reabsorption can be estimated using the formula for the transmission T_{FP} (ratio of transmitted intensity to the incident intensity) of a Fabry-Pérot interferometer at a transmission peak: $T_{FP} = T^2\exp(-\alpha L)/[1-R\exp(-\alpha L)]^2$. Here T = 1-R, where

#10797 - $15.00 US Received April 23, 1999; Revised June 15, 1999

T and R are the mirror intensity transmission and reflection coefficients, and $\alpha(t)$ is the time-dependent absorption coefficient of our 100-nm GaAs active layer. If the initial excitation density corresponds to transparency, $\alpha(0) = 0$ and $T_{FP}(0) = 1$. When the carriers have all disappeared, $\alpha(\infty)L \approx (1\ \mu m^{-1})(0.1\ \mu m) = 0.1$ and $T_{FP}(\infty) = 1.5\times10^{-3}$. This means that PL at the final stages of the decay is "shuttered" by three orders of magnitude compared with that in the beginning of the decay. Thus, the cavity-mode PL decays much faster than it would without this shuttering. This analysis is, of course, oversimplified; to get a quantitative description of shuttering and cavity enhancement effects including the shift of the cavity peak, we use a quantum theory where both spontaneous emission and reabsorption of photons are described microscopically.

The crucial role of guided modes in reducing the enhancement of the spontaneous emission rate in a planar microcavity was shown and emphasized by Lin et al. [21] and further illustrated by Abram et al. [23]. Reabsorption is an important consideration in the design of a resonant cavity light emitting diode [24]. De Neve et al. [25] modeled the light emission of a parallel-oriented dipole accounting for guided modes and quantum-well reabsorption. Even using only a single quantum well, they found that the mirror reflectivities needed to be less than 90% for good out coupling. They obtained an external quantum efficiency of ≈4% using ≈92% mirrors. By using very large diameter (1.5 mm) microcavities that guarantee that the guided mode light is reabsorbed and recycled they reached an external quantum efficiency of 20% [26].

In this work reabsorption distortion is avoided by collecting PL escaping through the top mirror without multiple reflections by using a ZnSe prism. For high-quantum-efficiency emission, clearly reabsorption must be avoided. In a resonant-cavity light emitting diode this is accomplished by keeping the active layer thin and the mirror reflectivity low. In a VCSEL this is accomplished by increasing the carrier density until the absorption is replaced by gain. The present technique permits one to observe the true carrier decay in a high-reflectivity cavity even when reabsorption is important. Thus it may be useful to study carrier dynamics and competition between guided-mode and cavity-mode emission in VCSELs below and around threshold.

2. Sample preparation and experimental technique for normal-incidence and steep-angle PL decay measurements

We studied a semiconductor microcavity with a 100-nm-thick layer of bulk GaAs. The microcavity structure, grown on a GaAs substrate by MBE, consists of a 1-λ $Al_{0.3}Ga_{0.7}As$ spacer between 22 pairs of top and 28.5 pairs of bottom distributed Bragg reflector (DBR) mirrors. Each low-index quarterwave mirror layer consists of 71.9 nm AlAs, and each high-index layer consists of a 12-period GaAs/AlGaAs superlattice whose effective index and Al composition are 3.46 and 19.5%, respectively. The reflectivity of both top and bottom mirrors is ≈99.9%. The layer of bulk GaAs is located at the antinode position of the standing wave whose wavelength is close to the wavelength at which the PL of bulk GaAs peaks at room temperature.

As shown in Fig. 1, a ZnSe prism with refractive index 2.89 and a bottom angle of 28° is glued to the top mirror of the semiconductor microcavity. At large internal angles, the mirror stop band shifts above the energies of the bulk GaAs PL emission, since the wavelength for maximum transmission of a Fabry-Pérot interferometer depends directly upon $\cos\theta$ where θ is the angle of observation relative to normal incidence. Thus the PL emitted at steep angles can escape through the second reflection dip below the mirror stop band. Without the prism, PL emitted at such steep angles undergoes total internal reflections and propagates along the direction parallel to the cavity plane as guided modes. [27,28] use a related technique.

The pump beam is incident on the microcavity with a small angle of 7° in the prism, so the scattering loss of the pump pulse at the glue layer between the surfaces of the prism and the top mirror is almost negligible. The wavelength of the pump pulse is tuned to the second

#10797 - $15.00 US Received April 23, 1999; Revised June 15, 1999

reflection dip above the mirror stop band, i.e., far above the GaAs band edge. The lifetimes for two different reflectivities of the top mirror are measured at approximately the same point, eliminating errors due to a possible positional dependence of the lifetime.

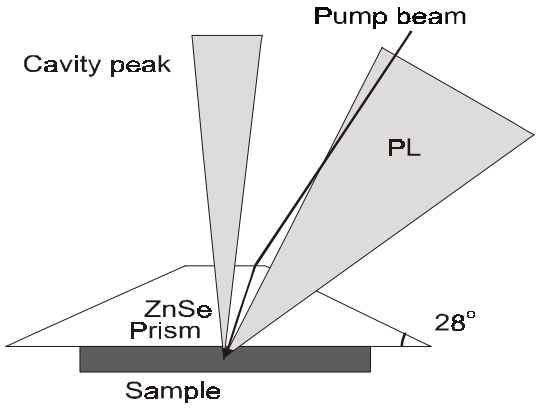

Fig. 1. Arrangement for pumping and detecting PL. A prism glued on the top of the sample permits the observation of PL that is free from multiple-layer interference; without the prism, it undergoes total internal reflection and goes into guided modes.

The collection lens is large enough to collect not only the PL emitted at steep angles but also cavity-mode PL emitted along the direction normal to the cavity plane as shown in Fig. 2 where both emissions contribute to the spectrum. The cavity peak is tuned to the lower energy side of the bulk GaAs PL to minimize reabsorption for cavity-mode light. This is done by first reducing the lattice temperature to 110 K and then decreasing the thickness of the spacer by scanning along the sample. For steep-angle PL decay measurements, the cavity-mode PL is blocked before it reaches the spectrometer.

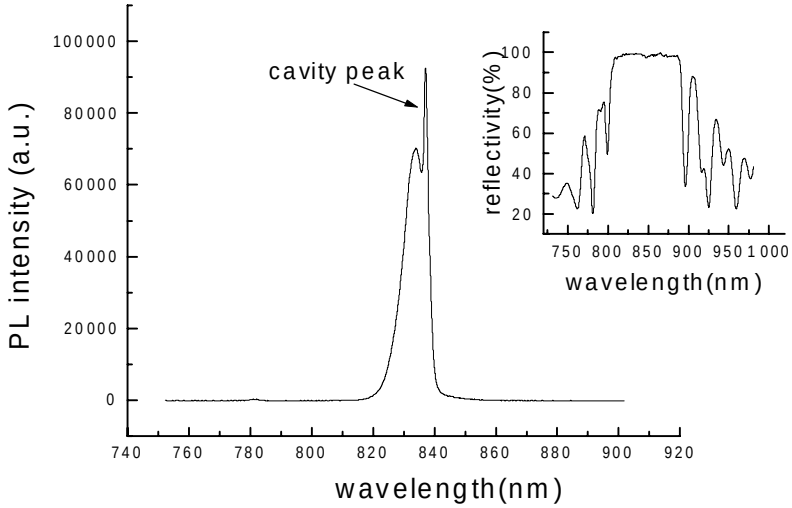

Fig. 2. The 110 K PL spectrum including both the emission by the cavity mode and emission at steep angles through the prism. A normal-incidence reflection spectrum of the sample measured at room temperature is shown in the inset.

After the ZnSe prism is glued to a 2-mm-square piece of the sample using crystal bond, the GaAs substrate is etched away. Then a series of measurements is performed with the full bottom mirror intact. Before the second series of measurements, all but ≈5 of the 28.5 pairs of the bottom mirror are etched away chemically. The reflectivity of the remaining bottom

#10797 - $15.00 US
Received April 23, 1999; Revised June 15, 1999

mirror is computed to be ≈78% near the cavity peak wavelength. The etch process is not as simple as for typical GaAs/AlAs DBR mirrors, because the high-index mirror layer consists of a GaAs/AlGaAs superlattice and the etch-rate selectivity between the superlattice and the AlAs layer is poor. Here, the etch rate for 1 period was calibrated accurately by etching test pieces repeatedly. The continuous flow of 1 part NH_4OH in 1000 parts 30% H_2O_2 for 2 minutes etches away both the superlattice layer and most of the AlAs layer. The remaining AlAs layer is etched by flowing 1 part 49% HF in 1000 parts H_2O for 20 second. The etching rate is quite dependent on the temperature of the etchant; both etchants were used at room temperature.

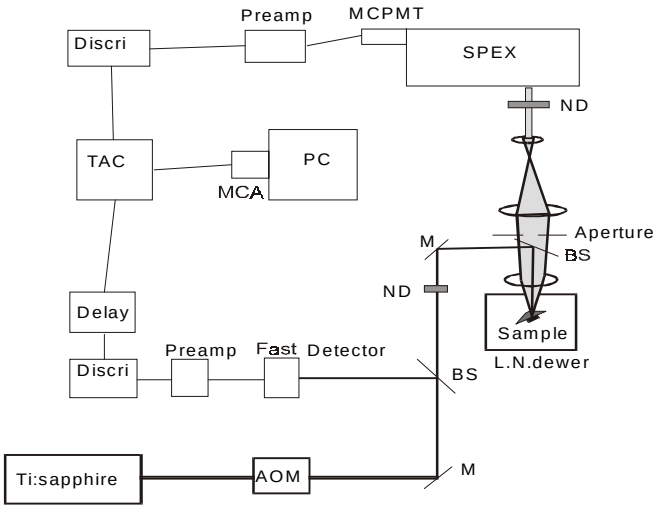

Fig. 3. Experimental setup for steep-angle PL lifetime measurements undistorted by reabsorption by the GaAs layer.

As shown in Fig. 3, measurements of the PL decay curve are performed using a time-correlated single-photon-counting technique. The pump source is a mode-locked Ti:sapphire laser (Tsunami). The pump wavelength, pulse length, and repetition rate are 783 nm, ≈100 fs, and 82 MHz, respectively. The spot size of our pump beam is measured to be ≈12 μm FWHM in free space. An acousto-optic modulator (AOM) is used to avoid thermal heating that causes a spectral shift of the emitted PL and decay-time distortion. The AOM gates on the pump pulses for 1 μs every 33 μs. A beam splitter separates the pump pulse into two beams. One beam is detected by a fast avalanche silicon photodiode whose output signal is amplified by a fast preamplifier, discriminated, delayed, and used as a stop signal for a time-to-amplitude converter (TAC). The other beam excites carriers in the sample. PL from the sample is filtered by a spectrometer (with output slit width wide enough to accept the entire PL spectrum) and detected by a fast microchannel photomultiplier tube. The output signal of the latter, after amplification and discrimination, goes to the TAC as a start signal. A multichannel analyzer and personal computer accumulate points to form a histogram of detected photons versus time. The time resolution of the system is about 200 ps. The counting rate is kept below 10^4 per second which is much smaller than the pulse repetition rate (approximately 2.5×10^6 per second after AOM gating). Since much less than one photon per pulse is detected on average, the PL kinetics is not distorted.

3. Experimental results and discussion

Our experimental results are summarized in Fig. 4. The decay times for the steep-angle PL emitted through the prism are shown in Fig. 4(a), where the two curves correspond to 28.5

#10797 - $15.00 US Received April 23, 1999; Revised June 15, 1999

and ≈5 periods of the bottom mirror. Removing all but five periods of the bottom mirror increases the PL decay time by ≈25%.

The PL decay time was extracted from the measured PL decay curve by a linear function fit: $\ln(I)=\ln(I_o)-t/\tau$. The two curves were measured at the same spatial position with an accuracy of about 10 μm. At first the decay times decrease rapidly with increased pump power, but then they stabilize and change quite slowly. (The cavity with only a five-period bottom mirror does not lase within our pump power range.) This insensitivity to the pump power is observed only with the steep-angle PL (emitted into directions that feed guided modes when the prism is absent). This indicates that carriers do not emit preferentially into cavity modes in the vicinity of lasing threshold.

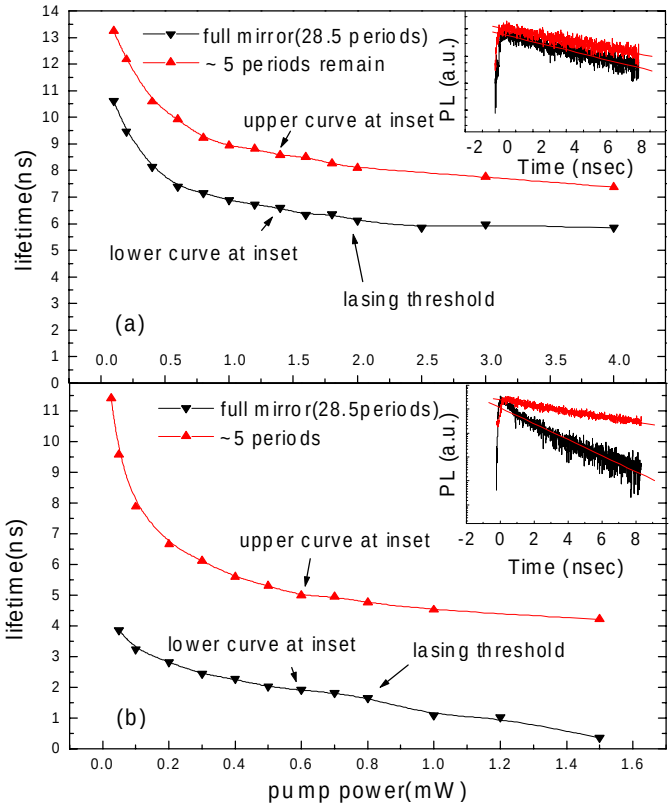

Fig. 4. PL decay times as a function of pump power at 110 K. (a) Decay times of steep- angle PL for two different reflectivities of the bottom mirror, ~78% and 99.9%. (b) Corresponding decay times of the cavity-mode PL emitted through the bottom mirror for the same mirror reflectivities.

Fig. 4(b) shows that the decay times of cavity-mode PL emitted through the bottom mirror, following normal-incidence pumping also through the bottom mirror, are significantly shorter than those for steep-angle PL in Fig. 4(a). The decay times measured with the bottom mirror complete are roughly 2.5 times shorter than those with a five-period bottom mirror. They are shorter than those in Fig. 4(a) for both mirror reflectivities.

Another difference is that a typical steep-angle PL decay curve, shown in the inset of Fig. 4(a), is very close to a single exponential, while that for the cavity-mode PL, inset of Fig. 4(b), is clearly nonexponential. Both insets are plotted in semilogarithmic scales, and the solid lines are linear-function fits.

The much faster decay of the cavity-mode PL can be attributed to the decreasing rate of photon escape from the cavity because of reabsorption by the GaAs layer whose absorption returns as the carrier density decays. Thus the cavity-mode PL can decay much faster than the

#10797 - $15.00 US
Received April 23, 1999; Revised June 15, 1999

square of the carrier density, as expected for radiative recombination of carriers in thermal equilibrium. Note that when reabsorption distortions are avoided there remains a small 25% enhancement of the decay rate as shown in Fig. 4(a). We expect no reabsorption distortion for the steep emission since the single-pass absorption is at most 10%, much less than the steep-angle transmission. The theory described below shows that this 25% increase is not a cavity-QED effect but faster emission into guided modes as mirror pairs are added.

When the cavity peak is located at higher energies than in Fig. 2, we obtained shorter cavity-mode PL decay times than in Fig. 4(b). These conditions and results are in agreement with Jin et al. [18], whose sample design was used to grow the sample studied here. Comparison of the high-reflectivity cases in Figs. 4(a) and 4(b) shows a decay time difference of more than a factor of two at low excitation intensities. This indicates that reabsorption shortens the cavity-mode decay time even for very low excitation intensities. It is now clear that the large cavity enhancement of the carrier decay rate reported in [18] is incorrect because the reabsorption-distorted cavity-mode PL decay was incorrectly assumed to follow $f_e f_h$. So far as we can ascertain, the same mistake was made in [20]. Further evidences for the importance of reabsorption in this high-reflectivity microcavity operated below lasing threshold are: the low top-emission quantum efficiency, discussed below; the time dependence of the cavity finesse; the angular dependence of the cavity-mode decay time; the wavelength dependence of the PL decay time; and the longer decay time for emission out a cleaved edge, in agreement with the steep-angle decay.

The very strong effect of a small amount of absorption upon PL due to reabsorption of photons emitted normal to the layers into a cavity mode was especially emphasized by Stanley et al. [29]. In analyzing a Fabry-Pérot interferometer containing a saturable absorber, Spiller [30] found that when the single-pass absorption increases to become comparable with the mirror transmission the interferometer's transmission drops drastically. Elimination of reabsorption by operating just below transparency is very difficult here because the unexcited single-pass absorption is so high (10%) and the mirror transmission is so low (<0.5%).

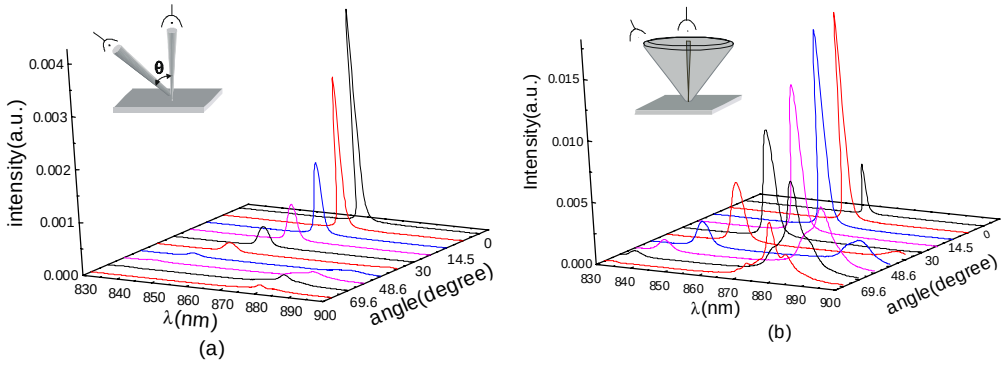

Fig. 5. Angular distribution of PL intensity emitted through the top mirror at room temperature (no prism). (a) Without and (b) with integration over the annulus shown in the inset.

4. PL angular distribution measurements

Fig. 5 shows the angular distribution of the PL emitted through the top mirror at room temperature. The measurements were performed on another piece of the same microcavity sample described above; neither mirror was etched. For the measurements shown in Fig. 5 (a) and (b), the emission was collected within a solid angle $\approx 7\pi \times 10^{-3}$ sr and focused into a single-mode fiber. Both the collection lens and the fiber were mounted on a rotating base that pivots about the position of the sample, thus emission into any angle within the plane of rotation (perpendicular to the microcavity plane) could be measured. The fiber throughput was

#10797 - $15.00 US
Received April 23, 1999; Revised June 15, 1999

focused into a scanning spectrometer followed by a PMT and lock-in-amp. The pump source was a cw Ti:sapphire laser.

Fig. 5(a) shows the spectrally resolved emission into an external angle θ for a carrier density of $\approx 10^{18}$ cm^{-3}. Varying the carrier density from $\approx 10^{17}$ cm^{-3} up to lasing threshold changes only the absolute magnitude of the data and not the relative size or spectral shape. Even with the pump power above lasing threshold, the spectral shape of the spontaneous emission at angles far from normal does not change. As θ increases from 0°, the amplitude of the emission peak decreases due to the decreasing finesse of the off-normal "cavity" and the changing overlap between the cavity resonance and the bulk GaAs PL spectrum.

Fig. 5(b) shows the integrated intensity of emission over the annulus that is created by rotating the solid angle subtended by the collection lens around the normal direction to the cavity. This numerical integration procedure allows us to directly compare the total intensity emitted in the normal direction to that coming out at larger angles. It shows that the intensity at the cavity resonance peaks at about 18°, dropping in half at about 5° and 40°. See Fig. 6.

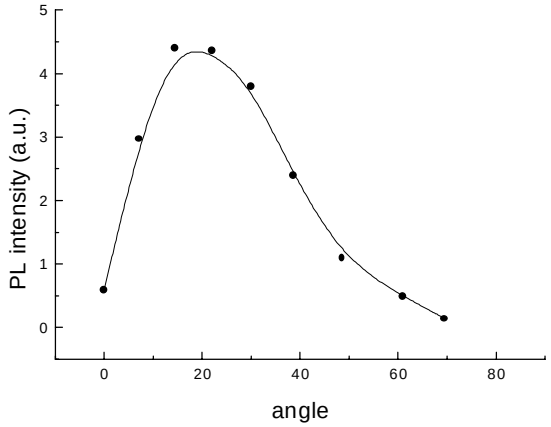

Fig. 6. Angular distribution of the PL intensity integrated over an annulus.

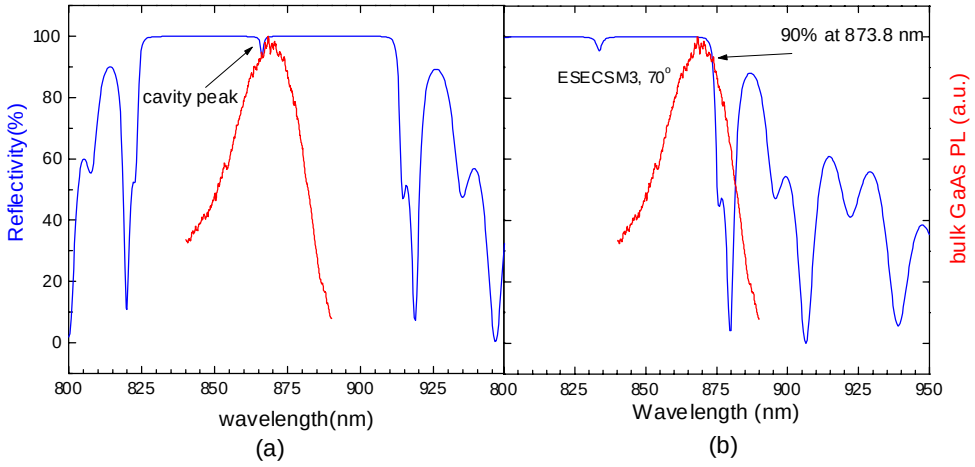

Fig. 7. The calculated spectral position of the cavity peak with respect to the bulk GaAs PL measured at room temperature for (a) θ=0° and (b) θ=70°.

At large angles, a second PL peak appears at longer wavelength. This occurs when the edge of the stop band shifts so high in energy with increased θ that the first reflection minimum below the stop band overlaps the PL spectrum. Fig. 7 shows the relative position of

#10797 - $15.00 US
Received April 23, 1999; Revised June 15, 1999

the cavity peak with respect to the PL spectrum of bulk GaAs at room temperature (a) for θ=0° and (b) for θ=70°. The angular distribution data were similar for two other samples with top (bottom) mirror reflectivities of 91% (96%) and 64% (85%), although the emission peaks were broader due to the lower finesses of the cavities. These lower-reflectivity samples emit much higher PL intensities and have larger quantum efficiencies (3.5 and 2.9%) than the high-reflectivity sample above (<< 1%). They have little if any enhancement of the carrier decay rate.

5. Microscopic analysis of electron-hole recombination rates

In the following we investigate, with the semiconductor luminescence equations [4,8-10], the microcavity enhancement of the electron-hole recombination rates observed in the experiments. Since the 100-nm bulk sample is still narrow compared to the light wavelength, the cavity enhancement effects are relatively insensitive to the thickness of the active material. Thus, we analyze the enhancement changes in a quantum well (QW) system, which considerably simplifies the microscopic investigations.

Our quantum theory of the interacting photon electron-hole system describes the quantum statistical features of the light by a boson operator $b_{\mathbf{q}}$ for each independent field mode $\mathbf{u}_{\mathbf{q}\sigma}(\mathbf{r})$ identified with a wave vector $\mathbf{q}$ and polarization direction $\mathbf{e}_{\mathbf{q}}$. For notational simplicity, we include the polarization index with $\mathbf{q}$. The quantum properties of the carrier system are determined by Fermion operators $e_{\mathbf{k}}$ and $h_{\mathbf{k}}$ for conduction band electron and valence band hole, respectively, having the in-plane momentum $\mathbf{k}$ [8].

For the incoherent excitation conditions used in the experiments, the light emission follows from the radiative recombination of incoherent electron-hole pairs leading to PL. The resulting emission and recombination properties can be determined from the dynamics of the photon number $\left\langle b^{\dagger}_{q_z,\mathbf{q}_{\|}} b_{q_z,\mathbf{q}_{\|}} \right\rangle$, where $\mathbf{q}_{\|}$ is the photon momentum in the QW plane, together with the electron occupation $f^{\mathbf{e}}_{\mathbf{k}} = \left\langle e^{\dagger}_{\mathbf{k}} e_{\mathbf{k}} \right\rangle$ and the hole occupation $f^{h}_{\mathbf{k}} = \left\langle h^{\dagger}_{-\mathbf{k}} h_{-\mathbf{k}} \right\rangle$. Due to the light-matter interaction, these expectation values are coupled via $\left\langle b^{\dagger}_{q_z,\mathbf{q}_{\|}} h_{-\mathbf{k}} e_{\mathbf{k}+\mathbf{q}_{\|}} \right\rangle$, describing the amplitude of photon assisted electron-hole pair recombination. The Heisenberg equations of motion for these quantities form the semiconductor luminescence equations,

$$i\hbar \frac{\partial}{\partial t}\left\langle b^{\dagger}_{\mathbf{q}} h_{-\mathbf{k}} e_{\mathbf{k}+\mathbf{q}_{\|}} \right\rangle = \left(\varepsilon_{\mathbf{k},\mathbf{q}_{\|}} - \hbar\omega_{\mathbf{q}} - i\gamma\right)\left\langle b^{\dagger}_{\mathbf{q}} h_{-\mathbf{k}} e_{\mathbf{k}+\mathbf{q}_{\|}} \right\rangle + \left(f^{e}_{\mathbf{k}+\mathbf{q}_{\|}} + f^{h}_{\mathbf{k}} - 1\right)\Omega_{\mathbf{k},\mathbf{q}} + f^{h}_{\mathbf{k}} f^{e}_{\mathbf{k}+\mathbf{q}_{\|}} \Omega^{SE}_{\mathbf{q}}, \quad (1)$$

$$\frac{\partial}{\partial t}\left\langle b^{\dagger}_{\mathbf{q},\mathbf{q}_{\|}} b_{\mathbf{q}',\mathbf{q}_{\|}} \right\rangle = i\left(\omega_{\mathbf{q}} - \omega_{\mathbf{q}'}\right)\left\langle b^{\dagger}_{\mathbf{q},\mathbf{q}_{\|}} b_{\mathbf{q}',\mathbf{q}_{\|}} \right\rangle + \frac{1}{\hbar}\sum_{\mathbf{k}}\left[F_{\mathbf{q}}\left\langle b_{\mathbf{q}'} e^{\dagger}_{\mathbf{k}+\mathbf{q}_{\|}} h^{\dagger}_{-\mathbf{k}} \right\rangle + F_{\mathbf{q}'}\left\langle b^{\dagger}_{\mathbf{q}} h_{-\mathbf{k}} e_{\mathbf{k}+\mathbf{q}_{\|}} \right\rangle\right], \quad (2)$$

$$\frac{\partial}{\partial t} f^{e}_{\mathbf{k}} = -\frac{2}{\hbar}\sum_{q,\mathbf{q}_{\|}} \mathrm{Re}\left[d^{*}_{cv} F_{\mathbf{q}}\left\langle b^{\dagger}_{\mathbf{q},\mathbf{q}_{\|}} h_{-\mathbf{k}-\mathbf{q}_{\|}} e_{\mathbf{k}} \right\rangle\right], \quad (3)$$

$$\frac{\partial}{\partial t} f^{h}_{\mathbf{k}} = -\frac{2}{\hbar}\sum_{q,\mathbf{q}_{\|}} \mathrm{Re}\left[d^{*}_{cv} F_{\mathbf{q}}\left\langle b^{\dagger}_{\mathbf{q},\mathbf{q}_{\|}} h_{-\mathbf{k}} e_{\mathbf{k}+\mathbf{q}_{\|}} \right\rangle\right], \quad (4)$$

where $\varepsilon_{\mathbf{k},\mathbf{q}_{\|}}$ is kinetic energy of the electron-hole pair with the Coulomb renormalization, $\omega_{\mathbf{q}}$ is the frequency of the field mode. We have evaluated the higher order correlation functions using a Hartree-Fock scheme and introduced a dephasing rate γ which is obtained from a separate calculation of correlation contributions in the second Born approximation [33]. The effective mode strength at the QW position is given by $F_{\mathbf{q}} = E_{\mathbf{q}}\int g(z)u_{\mathbf{q}}(z)dz$ with the QW

#10797 - $15.00 US Received April 23, 1999; Revised June 15, 1999

confinement function *g(z)* and the vacuum field amplitude $E_{\mathbf{q}}$. Equation (1) is driven by a spontaneous emission term,

$$\Omega_{\mathbf{q}}^{SE} = iF_{\mathbf{q}} d_{cv} \,, \tag{5}$$

where d_{cv} is the dipole matrix element. The electron-hole recombination is also altered by a renormalized stimulated process described by

$$\Omega_{\mathbf{k},\mathbf{q}} = d_{cv}\left[\sum_{q'} iF_{\mathbf{q}'}\left\langle b_{\mathbf{q}}^{\dagger} b_{q',\mathbf{q}_{||}}\right\rangle - \sum_{\mathbf{k}'} P d_{cv}^{*}\left\langle b_{\mathbf{q}}^{\dagger} h_{-\mathbf{k}'} e_{\mathbf{k}'+\mathbf{q}_{||}}\right\rangle\right] + \sum_{\mathbf{k}'} V_{\mathbf{k}'-\mathbf{k}}\left\langle b_{\mathbf{q}}^{\dagger} h_{-\mathbf{k}'} e_{\mathbf{k}'+\mathbf{q}_{||}}\right\rangle, \tag{6}$$

where the first two terms are the unrenormalized stimulated contributions. Here *P* defines the strength of the photon assisted polarization $\sum_{\mathbf{k}'} d_{cv}^{*}\left\langle b_{q}^{\dagger} h_{-\mathbf{k}'} e_{\mathbf{k}'+\mathbf{q}_{||}}\right\rangle$, and $V_{\mathbf{k}}$ is the quantum well Coulomb matrix element.

The recombination rate of each carrier density distribution is solved by evolving Eqs. (1) and (2) to steady state. The corresponding recombination rate γ_{eh} is obtained from Eqs. (3) and (4).

$$\gamma_{eh} = \frac{2}{\hbar S n_o} \sum_{\mathbf{k}} \sum_{q,\mathbf{q}_{||}} \mathrm{Re}\left[d_{cv}^{*} F_{\mathbf{q}} \left\langle b_{\mathbf{q},\mathbf{q}_{||}}^{\dagger} h_{-\mathbf{k}-\mathbf{q}_{||}} e_{\mathbf{k}} \right\rangle \right] , \tag{7}$$

where *S* is the cross sectional area of the QW and n_o is the carrier density. To evaluate γ_{eh} we have to first determine the mode functions corresponding to each **q**. For the structure used, the modal strength of the guided modes, propagating only inside the substrate or inside the cavity, highly exceeds the weight of modes which can propagate outside the cavity system. Thus, the recombination times are dominated by the PL into the guided modes.

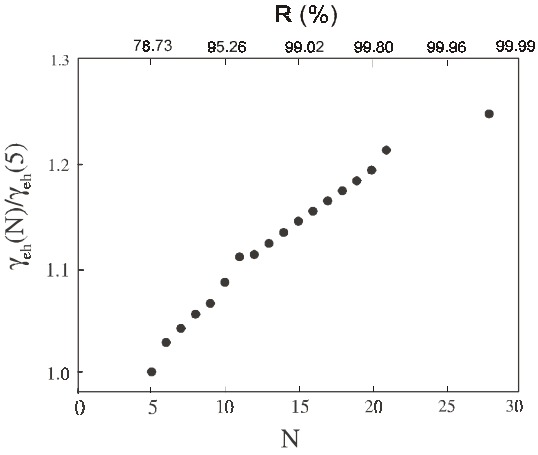

Fig. 8. Microscopically computed electron-hole recombination rates $\gamma_{eh}(N)$ for microcavities as used herein with different number N of quarterwave pairs in the bottom mirror. The top mirror has 22 pairs. A carrier density of 2×10^{11} cm^{-2} is assumed.

To determine the enhancement properties, we have computed γ_{eh} for a cavity similar to the experimental system such that the number of quarterwave pairs on the substrate mirror is varied from 5 to 28.5. The results in Fig. 8 show that γ_{eh} grows monotonically as a function of the number of pairs. According to the excitation conditions used in the experiment, we have used a carrier density $n_o = 2\times10^{11}$ cm^{-2} such that the system is below the lasing threshold but above the nonperturbative regime [9]. In this density range, the enhancement of γ_{eh} depends only weakly on n_o. For this excitation density, the cavity with 28.5 pairs enhances the

#10797 - $15.00 US
Received April 23, 1999; Revised June 15, 1999

recombination rates 25% compared to the 5 pair case as a consequence of a faster decay into guided modes. This result agrees with the experimental analysis performed through the prism. Thus, we conclude that the actual recombination times can be determined accurately using the prism method since the emission into a sufficient fraction of the guided modes is detected.

We have applied this theory to analyze the case of Yokoyama et al. [19]. Since they used three quantum wells in a low-index $\lambda/2$ spacer, reabsorption and guided-mode emission are much smaller than for [18,20], giving hope that they saw a real cavity-QED enhancement. Unfortunately, in their sample as well, guided modes govern the e-h recombination; their factor of two enhancement is again found to be caused by stimulated reabsorption which is strong when the PL is detected in the normal direction. Their full mirror enhances the rate by only 3%, because of the small refractive index of ZnS (2.2) and SiO_2 (1.5) in the top mirror; see Fig. 9.

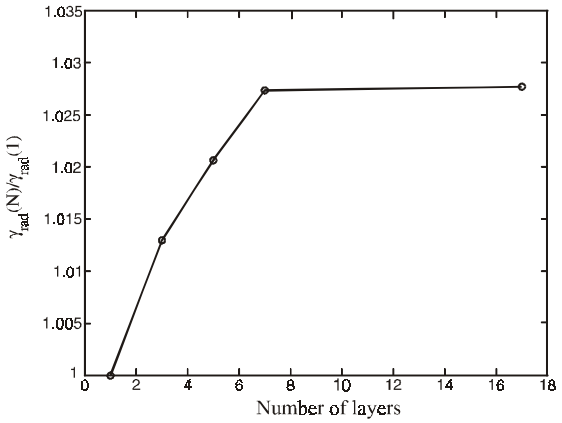

Fig. 9. Electron-hole recombination rate as a function of the number of layers in the top mirror of Yokoyama et al. [19], showing very little cavity-QED enhancement.

6. Summary

By comparing emission into steep-angle modes with the help of a prism with cavity-mode emission, we have shown that reabsorption makes the cavity-mode PL decay much faster. The large change in the decay rate of cavity-mode PL in a high-reflectivity microcavity is not a cavity-QED enhancement as previously claimed but is the consequence of reabsorption. The 25% decrease in the steep-angle PL decay rate when the substrate and all but five of the bottom mirror pairs are removed can be attributed to a change in the coupling into guided modes but not to cavity-QED. Lateral confinement to suppress guided modes seems to be the only way to force spontaneous emission into a single cavity mode [31,32,17]. It was shown in [34] that lateral optical confinement indeed can result in a spontaneous emission rate enhancement by a factor up to 5. We have developed a theory to compute electron-hole emission in a laterally confined microcavity that can be used to optimize the design of such structures for cavity-QED effects or LED quantum efficiency.

Acknowledgments

The Tucson group acknowledges support from NSF Lightwave Technology, DARPA/AFOSR, DARPA/ARO, and COEDIP and helpful discussion on mirror removal with W. Stolz. C. E. thanks the DFG for partial support. The Marburg group is supported by the DFG through the Sonderforschungsbereich 383, the Heisenberg Pogram (FJ), and the Leibniz Prize (SWK).

#10797 - $15.00 US Received April 23, 1999; Revised June 15, 1999